FAILURE ANALYSIS OF HINGED HOUSING ASSEMBLIES

Jeffrey A. Jansen, Stork Technimet, Inc.

Now with The Madison Group

Abstract

Failures occurred within medical housing assemblies. The cracking was observed in a significant number of parts that had been in service, and was found within the hinge bosses used on the various components of the assembly. The focus of this investigation was a determination of the nature and cause of the failures. The results obtained during the evaluation of the cracked components indicated that the failures occurred through slow crack initiation via fatigue and creep rupture mechanisms. This paper will review the testing performed to characterize the failure mode and identify the cause of the cracking, while demonstrating the analytical procedures used in the investigation.

Background

The housing assemblies were used in a medical application and the failures occurred within the hinges that secured the door and latch components to the main case body. Additionally, failures had also been reported within the corner of the latch component. All of the components were injection molded from Makroblend® EL-700, a polycarbonate/poly(ethylene terephthalate) (PC/PET) blend. The door and latch components were stated to have been molded using a family tool, with a separate molding operation used to produce the case. The housings were designed using an interference fit between the hinge pin and the hinge holes. Specifically, a 0.0495 inch hinge pin was used in conjunction with a 0.0480 inch diameter hole. In addition to the failed components, control parts and molding resin were also evaluated for reference purposes.

Experimental

Fracture surfaces of the cracked housing components were examined using a Hitachi S-3500N scanning electron microscope (SEM). The specimens were cleaned ultrasonically in a mixture of isopropanol and deionized water. Prior to the inspection the surfaces were gold sputter coated to enhance the imaging.

Residue samples were analyzed using energy dispersive X-ray Spectroscopy (EDS) using an Oxford Instruments Model 7021 system interfaced with the SEM.

Samples representing the failed assemblies were analyzed using micro-Fourier transform infrared spectroscopy (FTIR) in the attenuated total reflectance (ATR) mode. A Nicolet Magna 550 spectrometer interfaced with a Nic-Plan® IR microscope was used for the analysis.

Sample materials from the failed and reference assemblies were analyzed using thermogravimetric analysis (TGA). The testing was performed on a TA Instruments 2950 TGA system. The thermal program involved dynamic heating at 20 °C/min using sequential nitrogen and air purge atmospheres.

Materials representing the assemblies were evaluated using differential scanning calorimetry (DSC). The testing was conducted using a TA Instruments 2910 DSC. The analysis involved heating the samples at to a temperature above the melt transition, followed by controlled cooling through recrystallization. The same sample was then reheated at the same 10 °C/min rate, through the melting point.

Samples from the housing samples were analyzed using thermomechanical analysis (TMA). The testing was conducted using a TA Instruments 2940 TMA in conjunction with an expansion probe. The analysis involved heating the samples at 5 °C/min to a temperature above the glass transition under a nitrogen atmosphere.

The molecular weights of the assembly materials were evaluated indirectly by melt flow rate. The melt flow rate testing was conducted in accordance with ASTM D 1238 – Procedure B, using a temperature of 265 °C and a constant load of 5.0 kg.

Tests and Results

Visual Examination

Examination of the housing assemblies confirmed the presence of numerous cracks within both the door and latch hinges. The cracks were located in the latch and door hinges, made up of the case, door and latch hinge bosses. In general, the location and appearance of the cracks were consistent across all of the failed parts. Additional samples exhibited catastrophic failure within the corner of the latch.

The failed components were further examined with the aid of an optical stereomicroscope at magnifications up to 80X. The microscopic examination showed generally similar features across the failed components. The inspection did not reveal evidence of significant macro ductility, as would be apparent in the form of stress whitening, and permanent deformation. The cracks within the hinges, were present in both the door and latch hinge bosses, as well as the corresponding mating case hinge bosses, as illustrated in Figure 1. The cracks exhibited a continuous and regular appearance, suggestive of a single fracture front. Handling of the parts clearly showed that the cracks corresponded to areas of high stress. This was apparent in that hair-line cracks widened considerably upon closing the door and securing the latch. The cracks were completed in the laboratory and the fracture surfaces were examined microscopically. The crack surfaces, similar to the exterior portion of the housing components, did not show evidence

to suggest macro ductility, with the observed features being characteristic of brittle fracture. Specifically, no evidence was found to indicate yielding of the material, which suggested that the failures were associated with stresses below the yield strength of the material.

Examination of the parts that exhibited failure within the latch corner also revealed generally brittle features. The failures occurred within the corner of the part at a reinforcing rib designed with a relatively sharp corner. This area corresponded to the portion of the latch that makes contact with the door. Examination of the crack surface did not reveal signs of macro ductility, with the observed features being indicative of brittle fracture. The failures appeared to occur at an area on the latch which would be under the highest level of stress when engaged with the mating door.

A visual and microscopic examination of the reference case, door, and latch components did not reveal signs of pre-existing cracks. However, the components did exhibit knit lines from the molding operation. These knit lines, as shown in Figure 2, corresponded to the approximate location of the failures that had occurred within the case, door and latch hinge bosses. Based upon the examination of the submitted reference parts and the uniformity of the failures, representative components were selected for further evaluation.

Scanning Electron Microscopy

The fracture surfaces of typical failed components were further examined via scanning electron microscopy (SEM) in order to characterize the mode of crack initiation and extension. Examination of the fracture surface of one of the typical case hinge boss revealed features indicating that the cracking had initiated at both edges of the boss along the outer diameter, as represented in Figure 3. The crack origins exhibited a relatively smooth morphology, characteristic of brittle fracture associated with slow crack growth. No significant signs of micro ductility, as would be apparent in the form of stretched fibrils, were found within the crack origin locations. Areas remote to the origins exhibited additional signs of brittle fracture in the form of hackle marks and river markings. These features are normally associated with more rapid crack extension, indicating that the crack progressed relatively rapidly compared with the crack initiation step. The areas outside of the crack initiation zone exhibited evidence of limited micro ductility only at very high magnifications, as evidenced by the presence of stretched flaps.

Examination of the fracture surface of one of latch bosses revealed two distinct types of surface morphologies. The latch exhibited an area of crack initiation along the outer diameter edge of the component. This area exhibited features which were generally similar to those observed on the case fracture, including a relatively smooth surface lacking features indicative of significant micro ductility. Outside of the immediate crack initiation zone, increased levels of micro ductility were apparent in the form of stretched fibrils. Conversely, a second area of crack initiation was apparent on the opposite end of the hinge boss along the inner diameter of the hole. This area, as represented in Figure 4, exhibited substantial ductility at, and adjacent to, the crack initiation site. The observed features, including a nested pattern of stretched fibrils which were suggestive of failure via a low cycle fatigue mechanism, associated with the application of cyclic stresses. Thus, the latch boss fracture surfaces exhibited two distinct modes of crack initiation and extension, which produced catastrophic failure resulting from the union of the two individual fractures.

Examination of one of case boss fracture surfaces showed evidence of substantial micro ductility both within the crack initiation zone and the adjacent areas. The case exhibited a single crack initiation site along the inner diameter of the boss hole. The crack origin exhibited a high concentration of stretched fibrils. The morphology also included a nested pattern indicative of crack initiation and propagation through low cycle fatigue. Further evidence of ductility was found at areas adjacent to the crack origin. Locations remote to the crack origin also showed significant ductility. These remote locations, however, also exhibited hackle marks suggestive of more rapid crack extension.

Examination of the fracture surface representing the failure within the corner of the latch revealed features associated with crack initiation through brittle fracture. The crack origin area exhibited a relatively smooth morphology, with the presence of stretched fibrils only indicated at relatively high magnification. The crack origin was located along the inner diameter of the latch corner at an area representing a relatively sharp corner design feature. This fracture surface is shown in Figure 5. A slight increase in the ductility of the fracture surface was observed within a mid-crack area. Locations remote to the crack origin, along the outer diameter of the corner, showed relatively brittle fracture features associated with final mechanical overload of the component.

Throughout the examination of the boss fractures within the case and latch components, no evidence was found to indicate post-molding molecular degradation, such as chemical attack or thermal deterioration. Additionally, the observed features were not consistent with chemical interaction effects, such as environmental stress cracking (ESC) or solvation. In general, the observed features indicated cracking through two failure modes, creep and low cycle fatigue, associated with slow crack initiation. Areas remote to the fracture origins exhibited features, including hackle marks and river markings, indicative of more rapid crack extension. As such, it appears that the time to failure was principally established by the rate of the crack initiation step. The likely source of the stresses responsible for the creep and the fatigue failures is the

interference between the hinge pin and the hinge boss. This stress was applied both statically associated with creep and dynamically through repeated engagement of the latch via fatigue. The failure within the latch corner apparently originated at the inner diameter of the latch via brittle fracture. The relatively brittle fracture features observed within the crack origin relative to the mid-fracture zone are likely associated with severe stress concentration. This stress concentration was likely caused by the relatively sharp corner within the component causing apparent embrittlement of the latch.

Cross Sectional Examination

A cross section was prepared through a typical failed latch hinge to facilitate further examination of the cracking. The cross section was prepared by mounting a specimen in an epoxy media and subsequently polishing to reveal the areas of interest. An initial examination of the hinge within the latch boss revealed massive cracking within the component, as illustrated in Figure 6. The cross section revealed a significantly higher number of cracks than apparent from the external examination of the hinge. The cracks lacked features associated with apparent macro or micro ductility, and appeared to originate both within mid-wall areas and at the inner diameter immediately adjacent to the hinge pin. The general appearance of the fractures was consistent with cracks initiating through the exertion of stresses below the yield point for an extended period of time, via a creep mechanism. The sample was subsequently repolished in order to examine an area within the case hinge boss. Examination of the cross section revealed a significant level of cracking. The cracking closely resembled that observed within the latch boss. Catastrophic failure occurred at an apparent knit line, with additional cracking also present.

Fourier Transform Infrared Spectroscopy

Chemical analysis of the sample materials was performed using Fourier transform infrared spectroscopy (FTIR). Analysis of a sample of the molding resin produced a spectrum which exhibited absorption bands characteristic of both polycarbonate and a thermoplastic polyester, such as poly(ethylene terephthalate). Analysis of material representing the various assembly components produced results which produced a generally good match with the results obtained on the reference resin material. No evidence was found to indicate contamination of the failed component materials.

While a spectral comparison of all of the results obtained on the sample materials produced a reasonably good match, a minor variation was observed within spectral bands at 1239 cm^{-1} and 1227 cm^{-1}. Specifically, the failed component results showed a variation in the relative intensity of the bands, suggesting the presence of diphenyl carbonate. The presence of diphenyl carbonate is significant as it is a byproduct formed during the decomposition of polycarbonate resins.

Differential Scanning Calorimetry

Differential scanning calorimetry (DSC) of the molding resin generated results that were consistent with those expected for a polycarbonate/poly(ethylene terephalate) resin blend. The initial heating thermogram showed an endothermic transition at approximately 251 ºC, corresponding with the melting point of a poly(ethylene terephthalate) resin. This melting transition occurred at a lower temperature, 245 ºC, during the second heating run. This was in agreement with the expected behavior for a polycarbonate and poly(ethylene terephalate) blend, and is associated with the increased miscibility of the two individual polymers. The second heating run also showed two distinct glass transitions at 83 ºC and 140 ºC, associated with the poly(ethylene terephalate) and polycarbonate resins, respectively.

Analysis of a failed case at an area adjacent to the failed hinge boss produced results exhibiting melting endotherms at 250 ºC and 243 ºC during the initial and second heating runs, respectively. The results also showed the glass transitions associated with the poly(ethylene terephalate) and polycarbonate resins. As such, no evidence was found to indicate contamination of the case material. Significantly, the initial heating run results also showed an exothermic transition centered at approximately 123 ºC, as illustrated in Figure 7. This is associated with low temperature crystallization of the poly(ethylene terephalate) resin, and represents undercrystallization of the material in the as-molded condition.

Thermogravimetric Analysis

Thermogravimetric analysis (TGA) of the resin and housing components was performed to further evaluate the compositions of the samples. The testing produced consistent results across all of the analyzed samples. All of the obtained thermograms showed a minor weight loss at relatively low temperatures associated with the evolution of volatile materials. At higher temperatures under a dynamic nitrogen purge, the results exhibited the primary weight loss step associated with the decomposition of the polymer. The weight loss step associated with the initial decomposition of the polymer included a leading edge shoulder and a general bimodal pattern, consistent with the presence of a flame retardant. A third weight loss, associated with the combustion of char formed during the initial decomposition of the polymer, occurred at elevated temperatures under an air atmosphere. Upon conclusion of the evaluation, a non-combusted residue content of approximately 3.0% was obtained. The TGA results obtained on the analyzed samples were consistent with those expected for a flame retardant grade of a polycarbonate/poly(ethylene terephalate) resin blend.

Energy Dispersive X-ray Spectroscopy

The residue remaining after the TGA evaluation of the resin sample was analyzed using energy dispersive X-ray spectroscopy (EDS). The results, as presented in Table 1,

showed that the TGA residue consisted of relatively high concentrations of titanium and oxygen, with lesser amounts of carbon, sodium, aluminum, silicon, phosphorus and potassium. The obtained results were consistent with titanium dioxide, a white pigment commonly used in plastic resins. The presence of this material is significant, however, as polycarbonate resins are known to be degraded by titanium dioxide[1].

Thermomechancial Analysis

Thermomechanical analysis (TMA) of specimens excised from the hinge bosses of failed case and latch components was performed to evaluate and compare the physical properties of the part samples. The results showed a similar response to the thermal program, with the samples initially expanding in a steady, linear manner. This linear expansion continued through 105 to 130 ºC, upon which the samples lost load bearing capabilities and contracted. This temperature was consistent with the glass transition temperature of the polycarbonate and represents the inability of the material to withstand loads. It is significant to note that upon reaching the glass transition temperature, none of the samples exhibited rapid expansion, which is indicative of substantial molded-in stresses within the component materials.

Melt Flow Rate

The melt flow rate of the material was determined as a mean to assess molecular weight. The melt flow rate test results, as presented in Table 2, indicated that the resin sample produced an average melt flow rate of 15.6 g/10 min. This is in excellent agreement with the published nominal value of 16 g/10 min. and the corresponding specification of 10 g/10 min. to 20 g/10 min. for the resin. The results obtained on molded parts showed a significant increase in melt flow rate relative to the resin. Because of the inherent impact resistance of the material, a shift of approximately 50%, frequently results in functional parts. However, an increase of less than 40% from resin to parts is preferred. The increases observed in the failed parts was severe and cannot be considered as satisfactory, even if the lot of material used to produce the parts was at the high end of the specification range. The observed level of increase in the melt flow rate and the corresponding reduction in the molecular weight of the failed parts is consistent with the apparent brittle nature of their performance. As molecular weight is reduced through degradation, all material properties including strength, impact resistance, creep resistance and fatigue resistance are reduced. The relative widespread variation obtained during the melt flow rate testing is consistent with the reported adjustment in the molding process. Given the obtained results, it appears that the current process is superior to the previous processes in retaining the molecular weight of the molding resin.

During the melt flow rate testing, the samples were dried at 100 ºC under vacuum. As a result of this, the color of the materials had a tendency to darken. There was a direct correlation between the extent of the color change and the determined melt flow rate. The virgin material and the lower melt flow rate parts showed only a small color shift, while the parts in the high melt flow rate range displayed a significant color shift. This suggests that higher levels of degradation produced chemistries that are prone to color formation at elevated temperatures.

Conclusion

It was the conclusion of the investigation that the cracking and failures observed within the housing assembly hinges occurred through two primary mechanisms. The visual, microscopic, and SEM examinations indicated that the cracking initiated within the hinge bosses through low cycle fatigue, and through the exertion of relatively low stresses below the yield points over an extended period of time via a creep mechanism. In both the fatigue fracture and the creep ruptures, the crack initiation step appeared to take place relatively slowly, as indicated by the observed fracture features. In both mechanisms, the stresses thought to be responsible for the failure are associated with the interference between the hinge pin and the hinge boss. This is consistent with the stated interference fit between the pin and the hole. The creep failures were induced by the static stresses resulting from the interference fit and the rigidity of the assembly, thus transferring all of the component stress to the hinges. The fatigue failures are thought to result from the same stresses being applied repeatedly, with an increase in the stress level produced by the latching operation. Engagement of the latch onto the door demonstrated a distortion of the apparent cracks within the hinge area. Cracking within the hinge boss of the case, door and latch components initiated at both the inner diameter and outer diameter of the holes. The crack origin site is determined by the areas which are under the highest level of stress, or the areas which are inherently weak. In general, the fracture locations corresponded to areas of knit lines within the components. Knit lines are often associated with localized areas of poor fusion and are commonly the weakest area of the molded part.[2] While the knit line areas exhibited catastrophic failure, the cross sectional examination indicated massive cracking within the boss. The observed cracking was consistent with stress fractures, as would be caused by the exertion of stresses below the yield point over an extended period of time.

Evaluation of the failures that occurred within the corner of the latch showed that the cracking initiated at a relatively sharp corner within the component design. Relatively sharp corners produce severe stress concentration in plastic components. This stress concentration compounded the

1 Titanium Dioxide Induced Failure in Polycarbonate, M. Blackwood, R. A. Pethrick, F. I. Simpson, R. E. Day and C. L. Watson Journal of Materials Science Volume 30, Number 17 / September, 1995. p. 4435-4445

2 Failure Analysis Case Studies**,** Part I: Effect of Processing Conditions and Part Design**,** Elleithy. R, **(**ANTEC), 1999

stresses placed on the part by the engagement of the latch and door components.

In summary, the failures that occurred within the hinge components were the result of static and dynamic stresses placed on the part during service and opening and engagement of the door/latch system. These stresses resulted in creep and low cycle fatigue failures initiating at both the outer diameter and inner diameter areas of the case, door and latch hinge bosses and within the corner of the latch. While the source of the stress is clearly evident, additional factors appear to be significant to the failures.

The analysis of the submitted resin material produced results characteristic of an unfilled, flame retardant grade of a polycarbonate/poly(ethylene terephalate) resin blend. These results are consistent with the indicated material, Makroblend® EL700. Analysis of the failed and submitted reference parts produced results which were generally consistent with those obtained on the resin. No evidence was found to indicate contamination of the resin material. However, the melt flow rate testing, and to a lesser degree the FTIR analyses, indicated massive degradation within the failed part components. Given the nature and application of the components, this degradation is thought to be associated with the molding operation. Specifically, three aspects of the production process could result in molecular degradation of the resin. The least likely of these is degradation during the drying of the resin. If degradation had occurred during the drying process, it is likely that significant discoloration would have been observed within the molding resin. Another aspect of the production which could cause degradation is the exposure of the material to elevated temperatures for a prolonged period of time in the melt state while the material is in the injection molding barrel. The final, and most likely cause of the degradation, is improper drying of the material, such that the material contained too much moisture at the time of molding. Makroblend® resins need to be dried to a moisture content below 0.02%, with recommendations often indicating a moisture content less than 0.01%. If the resin is not properly dried, exposure to elevated temperatures can result in hydrolysis of the polymer.

During the evaluation of the failed components, it was also observed that the resin had been undercrystallized during the molding operation. Undercrystallization is often the result of molding in a relatively cold tool, thus producing a frozen-in amorphous region within the preferentially crystalline structure of the material. Reduced crystallinity can have a significant impact on the properties of the molded article. In general, reduced crystallinity can result in a reduction in the tensile properties, as well as a loss in creep resistance and fatigue resistance.

A third factor which could affect the performance of the molded component is the relatively high level of titanium dioxide within the pigmented resin. A non-combustible residue of approximately 3.0% was obtained during the TGA analysis and elemental analysis of this residue determined it to be principally titanium dioxide. Titanium dioxide is known to produce degradation during molding in polycarbonate-based resins.

The presence of a knit line within the hinge bosses is also considered a significant factor in the failures. However, the presence of cracking outside these areas was also indicated. Design issues are also thought to be involved in the failures. The level of stress imparted by the interference fit between the hinge boss and pin is substantial, and is considered the driving force behind the cracking. The failure within the latch corner is attributed to severe stress concentration caused by an insufficient radius within the part design. Throughout the evaluation, no evidence was found to indicate that chemical affects such as molecular degradation or environmental stress cracking played a role in the failure.

Ongoing Investigation

Pursuant to the failure investigation two additional studies are being conducted. Sample representing different types of housing components are being evaluated in order to evaluate the mechanical strength of the molded-in hinges. Additionally, components are being tested order to assess and compare the levels of internal stress within the assembled components.

Keywords

failure analysis, fatigue, creep

Table 1
EDS Results
(relative weight percent)

Element	TGA Residue
Silicon	0.5
Aluminum	0.5
Sodium	0.2
Potassium	0.1
Titanium	43.6
Phosphorus	0.2
Carbon	9.3
Oxygen	45.7

Table 2
Melt Flow Rate [1]
(g / 10 min)

Results	Resin	Failed Door	Failed Case
Average	15.56	69.06	76.15
Change vs. Resin [2]	---	+344%	+389%

[1] Testing performed at 265 ºC with a 5 kg load
[2] Based upon a resin value of 15.56 g/10 min.

Fig. 1 - Cracking was present within the housing assembly

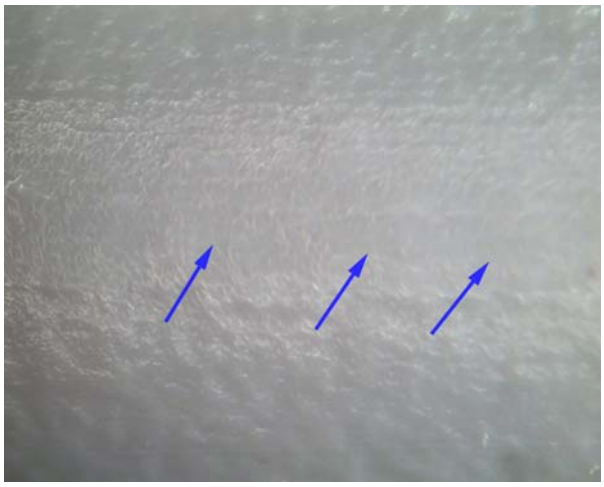

Fig. 2 - A knit line was present on the hinge component.

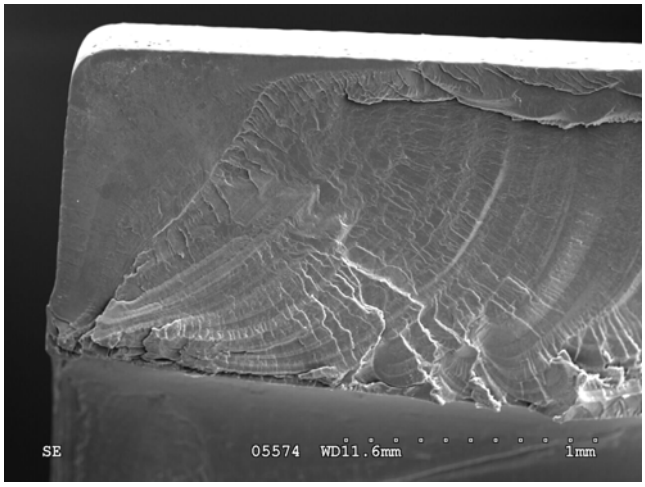

Fig. 3 - Scanning electron image showing a typical hinge boss fracture surface. The crack origin region displayed a smooth morphology

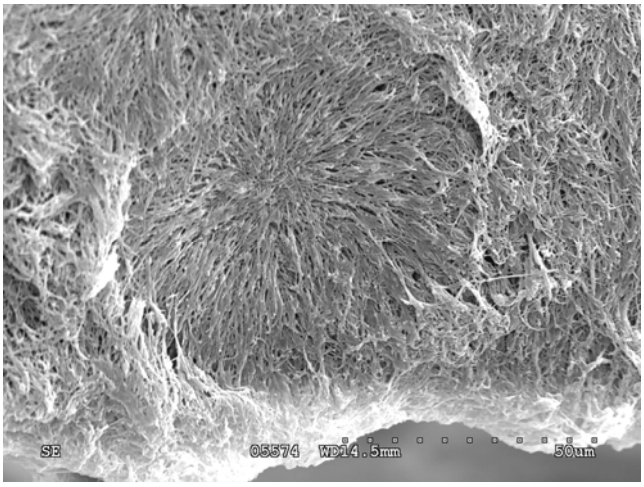

Fig. 4 - Scanning electron image showing features associated with low cycle fatigue on the fracture surface.

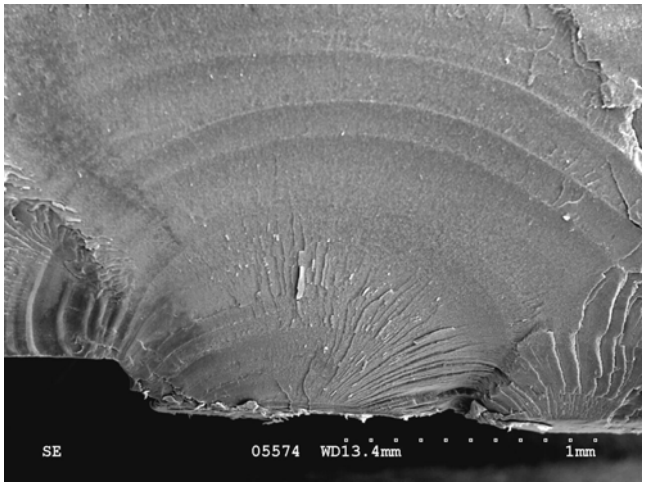

Fig. 5 - Scanning electron image showing a typical fracture surface on a corner latch failure. Arrest markings are evident.

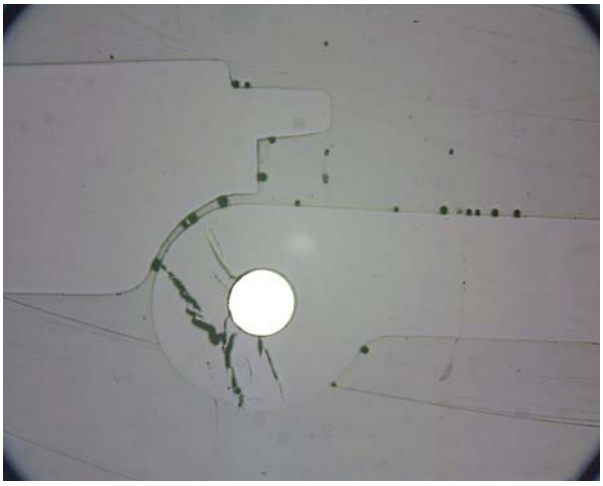

Fig. 6 - The cross sectional examination revealed the presence of massive cracking within the hinge bosses.

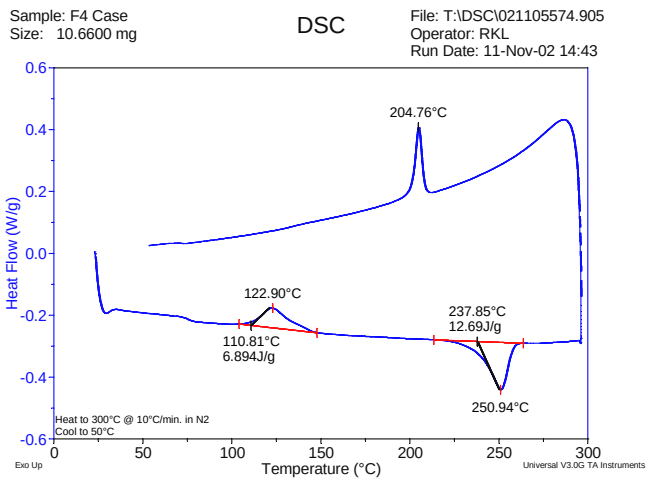

Fig. 7 - DSC thermogram obtained on the failed part material.

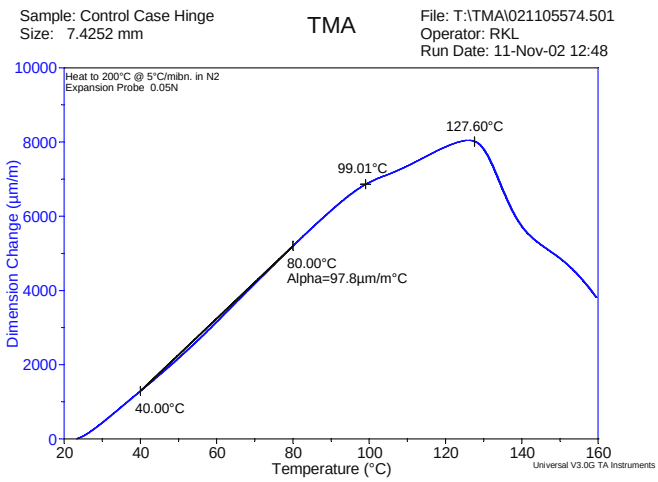

Fig. 8 - TMA thermogram obtained on the failed part material.